Contents lists available at ScienceDirect

Regional Studies in Marine Science

Metabolic significance of temperature-dependent changes in annual resolution coral δ^{13}C from the South China Sea during the mid-Holocene

Yangrui Guo [a,b,c], Wenfeng Deng [a,c,*], Gangjian Wei [a,c], Hangfang Xiao [a,b,c], Xuefei Chen [a,c]

[a] State Key Laboratory of Isotope Geochemistry, Guangzhou Institute of Geochemistry, Chinese Academy of Sciences, Guangzhou 510640, China
[b] College of Earth and Planetary Sciences, University of Chinese Academy of Sciences, Beijing 100049, China
[c] Southern Marine Science and Engineering Guangdong Laboratory, Guangzhou 511458, China

ARTICLE INFO

ABSTRACT

The complicated effects of climatic and environmental conditions on coral δ^{13}C have hindered its use as a universal proxy for biological activity and climate change. Changes in annual resolution δ^{13}C levels from the South China Sea (SCS) were studied to explore the biological and climatic significance of coral δ^{13}C during the mid-Holocene. The growth-rate-related kinetic isotope effect on modern coral δ^{13}C may be limited, site- and/or colony-specific. Furthermore, coral δ^{13}C and sea surface temperatures (SST) are inversely related, but their correlation is weak. These results suggest the influence of complicated controlling factors on modern coral δ^{13}C. As for the mid-Holocene corals, no obvious growth-rate-related kinetic isotope effect has been found in their coral δ^{13}C series, and the effect of solar irradiation on coral δ^{13}C is difficult to directly evaluate for the low resolution of reconstructed solar records and the dating errors. However, mid-Holocene coral δ^{13}C series show temperature-dependent changes over the studied periods during 6100–6500 yr BP. The significant negative correlation between coral δ^{13}C and SST has been attributed to the high SSTs during the mid-Holocene. This is based on the observation that coral δ^{13}C and the photosynthesis to respiration ratio (P/R) are usually positively related, but P/R is significantly and negatively related to temperature under high temperature conditions in that photosynthetic activity of heat-stressed corals will drastically reduce due to the decreases of population density and photosynthetic rate of the zooxanthellae.

© 2019 Elsevier B.V. All rights reserved.

1. Introduction

Coral reefs have the highest productivity and biodiversity of any ecosystem in the world's oceans (Knowlton et al., 2010); however, they face increasing threats from rising sea surface temperatures (SST) and ocean acidification (Hoegh-Guldberg et al., 2007; Hughes et al., 2017; Lam et al., 2019) that may lead to their eventual extinction (Carpenter et al., 2008). The ability of coral reefs to adapt their calcification process to global warming and ocean acidification may be one of the most important factors determining their future. Recent studies suggest that coral reefs may possess the biological properties of resilience and acclimatization with respect to climate change stressors (McCulloch et al., 2012, 2017; DeCarlo et al., 2018). For example, corals can interactively up-regulate the dissolved inorganic carbon (DIC) and pH of their calcifying fluid to maintain stable calcification rates in changing

ocean environments (McCulloch et al., 2017). Even so, it is not clear whether coral reefs will be able to survive under a regime of continuously increasing temperatures and ocean acidification. Model simulations can provide theoretical predictions that can be used to address this question (Hoegh-Guldberg et al., 2007). However, most models have inherent weak points such as subjectivity and inappropriate methods (Buddemeier et al., 2008). Consequently, historical reconstructions of the metabolic activity of coral reefs are likely to be a supplementary alternative to generate realistic estimates of their potential future development in a changing world (Kittinger et al., 2011).

Symbiotic coral skeleton carbonate formation results from the delivery of Ca^{2+} and DIC to the site of calcification, and the major source of DIC is metabolic CO_2 (50%–90% of total $CaCO_3$ deposition), and 10%–50% originates from the seawater carbon pool (Goreau and Yonge, 1977; Erez, 1978; Furla et al., 2000). The metabolic CO_2 is closely associated with metabolic activity such as respiration and photosynthesis; therefore, carbon isotope fractionation (δ^{13}C) in symbiotic coral skeletons is believed to be predominantly influenced by metabolic processes (Grottoli, 2000) and could be used to reconstruct biological activities such

as coral polyp respiration, endosymbiotic zooxanthellae photosynthesis, heterotrophic feeding, growth rate and coral spawning (Gagan et al., 1994; Swart et al., 1996; McConnaughey et al., 1997). However, the very complicated effects of climatic and environmental conditions on coral $\delta^{13}C$ have hindered its use as a universal proxy for biological activity and climate change. Seasonal variations in coral $\delta^{13}C$ are controlled by a wide range of different factors, such as solar radiation, cloud cover, rainfall, terrestrial DIC input and human activity (Moyer and Grottoli, 2011; Deng et al., 2013; Xu et al., 2018), but the secular declining trend in coral $\delta^{13}C$ levels over the past 200 years reflects the increase in the transfer of ^{12}C-enriched anthropogenic CO_2 from the atmosphere to the surface oceans (Swart et al., 2010; Dassié et al., 2013; Liu et al., 2014; Deng et al., 2017), and the centennial-scale variations of coral $\delta^{13}C$ before the industrial revolution over the past millennium are believed to record the evolution of total solar irradiance affecting the photosynthetic activity of the endosymbiotic zooxanthellae (Deng et al., 2017). Even so, the biological and climatic significance of coral $\delta^{13}C$ in fossil corals older than a thousand years is rarely studied (Deng et al., 2013).

Global SST rise is accelerating (Bâki Iz, 2018), and the future of coral reefs under rapid climate change are widely concerned (Chen et al., 2016; Hoegh-Guldberg et al., 2017; Camp et al., 2018; Chen et al., 2018; Lough et al., 2014) . The reconstruction of coral biological activity from a historical period much warmer than the present may help us to predict the likely response of coral reefs to a warming climate. In this regard, the mid-Holocene (roughly 7000–5000 yr BP) is an ideal choice for such a study. During the Holocene Megathermal (also known as the Holocene Climatic Optimum; Shi et al., 1993), temperatures in many places on Earth, including continents and oceans, were higher than or close to the present (e.g., Shi et al., 1993; Gagan et al., 1998; Hewitt and Mitchell, 1998; Axford et al., 2013; Lough et al., 2014; Samartin et al., 2017). Given that coral reefs are widely distributed across the South China Sea (SCS) and the developmental history of reefs there can be dated back to the early Miocene or late Oligocene (Yu, 2012), our study site is an excellent place to carry out such a reconstruction. Moreover, in the SCS during the mid-Holocene around 6000 yr BP, SSTs were higher and seawater pH values were equivalent to, or even lower than present day values (Wei et al., 2007; Liu et al., 2009).

In this study, we present three annual-resolution coral $\delta^{13}C$ records from the northern SCS from the period 6100–6500 yr BP, each of which is around 40 years long. Because of the complication and debate of seasonal $\delta^{13}C$ mentioned above, we studied changes in annual resolution coral $\delta^{13}C$ to explore the biological and climatic significance of coral $\delta^{13}C$ during the mid-Holocene.

2. Materials and methods

Three mid-Holocene coral cores (SYL-4, SYL-1-3, and SYO-15) were recovered from separate *Porites* colonies on the fringe reef in Dadonghai Bay, Sanya on southern Hainan Island in the northern SCS (Fig. 1), and were dated to 6217 ± 29 yr BP, 6342 ± 19 yr BP, and 6494 ± 24 yr BP, respectively (Wei et al., 2007). The sample preparation and pretreatment methods were referred to Wei et al. (2007). Analysis of the Sr/Ca ratios was performed on a Varian Vista Pro inductively coupled plasma optical emission spectrometry, and the standard reference material used for calibration was the JCp-1 *Porites* sp. standard (Okai et al., 2012). Replicate analyses of an in-house *Porites* sp. coral standard solution showed an external precision of 0.16% yielding a SST error of less than 0.5 °C. Coral skeletal $\delta^{13}C$ and $\delta^{18}O$ analysis was conducted using a GV Isoprime II stable isotope ratio mass spectrometer coupled with a MultiPrep carbonate device that used 102% H_3PO_4 at 90 °C to extract CO_2 from the coral samples, following the procedures
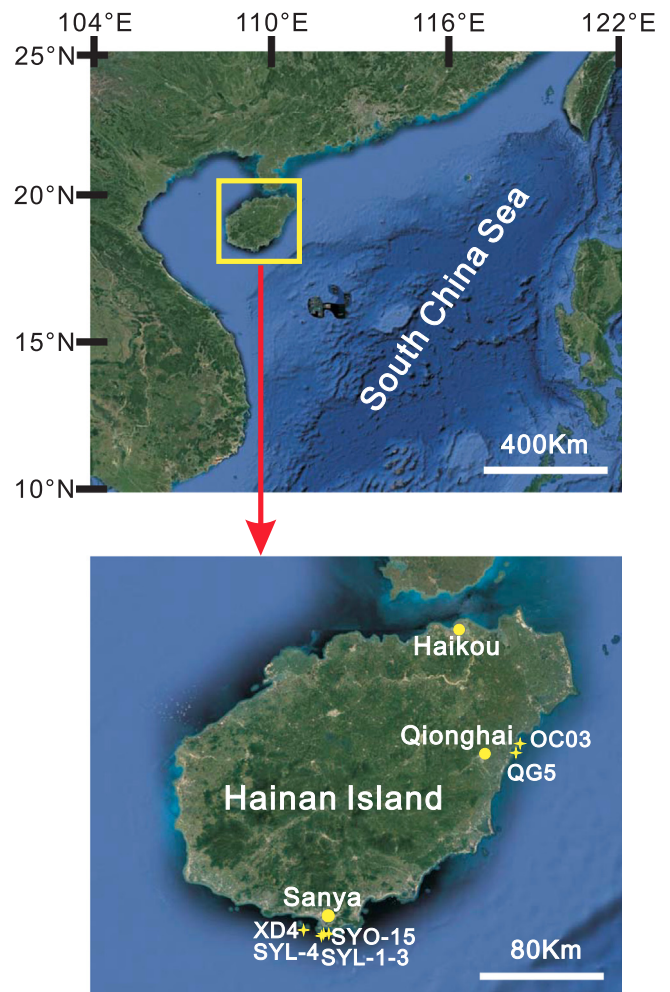

Fig. 1. Satellite image of Hainan Island and the SCS. Yellow stars indicate sampling locations.

described by Deng et al. (2009). Isotope data were normalized to Vienna Pee Dee Belemnite (V-PDB) using the NBS-19 standard ($\delta^{13}C = 1.95‰$, $\delta^{18}O = -2.20‰$). Multiple measurements on this standard yielded a reproducibility of 0.03‰ for $\delta^{13}C$ and 0.06‰ for $\delta^{18}O$. Replicate geochemical measurements were made on approximately 15% of the samples.

Seasonal changes in the Sr/Ca, $\delta^{18}O$, $\Delta\delta^{18}O$ and $\delta^{13}C$ values of these corals have been used previously to study SST, the timing of the rainy season, and sea surface salinity during the mid-Holocene (Wei et al., 2007; Deng et al., 2009; Guo et al., 2016), as well as the environmental controls on seasonal changes in coral $\delta^{13}C$ (Deng et al., 2013). We used the data from three modern corals published by Sun et al. (2008) for comparison. Of these, samples QG5 and OC03 were collected from two live *Porites* colonies offshore from Qionghai, Hainan Island, and sample XD4 was collected from another live *Porites* colony on Xidao Island in the northern SCS (Fig. 1). The changes in these three modern coral $\delta^{13}C$ series have been used previously to study the effects of photosynthesis, respiration, and human activity on monthly resolution coral $\delta^{13}C$ (Sun et al., 2008). The detailed sampling information for all corals can be found in the previous studies referred to above.

To study changes in annual resolution coral $\delta^{13}C$ in the mid-Holocene corals, the monthly $\delta^{13}C$, SST and $\Delta\delta^{18}O$ (reconstructed from the Sr/Ca and $\delta^{18}O$ ratios) were first converted into annual mean changes by averaging the 12 months of data from each

chronological year. The chronological years were constructed using the Sr/Ca ratios, which track changes in the ambient water temperature, and by assuming that each Sr/Ca cycle represents one year. Maxima in Sr/Ca ratios were assigned to the beginning of each year, which is generally the coldest period in this region. The monthly data from each chronological year were obtained by linear interpolation (for an annual cycle with <12 data points) or nearest neighbor smoothing (for an annual cycle with >12 data points) in each Sr/Ca cycle assuming the linear growth of corals (Deng et al., 2013). The annual growth rates of the mid-Holocene corals were estimated from the product of the sampling number in each chronological year and the sampling interval (0.8 mm). Most studies used the breadths of annual density bands in X-radiographs of thin cross-sections of coral skeletons to measure annual growth rates (Gustafson, 2006). Considering the sub-samples were collected from annual bands along the main growth axis using a digitally controlled milling machine and the sampling intervals are *strictly equal*, the method for growth rate estimation should be reliable. The annual mean δ^{13}C and growth rates of the modern corals, as well as the instrumental SST records, were obtained from Sun et al. (2008).

3. Results

The annual mean δ^{13}C and growth rates of the modern corals, as well as the instrumental SST records, are presented in Fig. 2. Considering the analytical error of 0.03‰ for δ^{13}C, the δ^{13}C of all three modern corals shows a significant declining trend during their respective growth periods (Fig. 2a). Their growth rates follow an increasing trend at a measurement accuracy of about 1 mm, but this trend is not significant for the coral XD4 (Fig. 2b). At the same time, the SSTs in the three sampling locations increased gradually over the study period (Fig. 2c).

The annual δ^{13}C, $\Delta\delta^{18}$O and growth rates of the mid-Holocene corals, as well as the SST records retrieved from coral Sr/Ca, are presented in Fig. 3. For the fossil coral SYO-15, its δ^{13}C shows a continuous declining trend from −1.45‰ to −2.40‰ over the period 6494–6460 yr BP (Fig. 3a), whereas the SST over the same period increases gradually from 28.3 °C to 29.9 °C (Fig. 3d). The trends in δ^{13}C seen in the other fossil corals, SYL-1-3 and SYL-4, were not continuous but fluctuated (Fig. 3a), and those of the SSTs during their growth periods (ca. 6340–6298 and 6215–6174 yr BP, respectively) were also oscillatory (Fig. 3d). The annual $\Delta\delta^{18}$O and growth rates of these three mid-Holocene corals showed no obvious long-term trends (Fig. 3b and c).

## 4. Discussion

4.1. The growth-rate-related kinetic isotope fractionation effect and its impact on coral δ^{13}C

Previous studies have indicated that kinetic fractionation related to changes in growth rate has a major effect on the δ^{13}C levels preserved in coral skeletons, and some studies have reported a significant inverse correlation between coral δ^{13}C and the linear growth rate (McConnaughey, 1989; Allison et al., 1996; Suzuki et al., 2005). However, other studies have found no relationship between growth rate and coral δ^{13}C (Swart et al., 1996; Deng et al., 2017), and corals growing as slowly as 1.5 mm/yr had essentially identical δ^{13}C values to portions of the same coral growing at rates of up to 8 mm/yr (Swart et al., 1996). In addition, a declining trend in the growth rates of massive *Porites* corals in the SCS and adjacent areas has been recorded in recent years (Tanzil et al., 2013; Su et al., 2016); consequently, the growth-rate-related kinetic isotope fractionation effect and its impact on SCS coral δ^{13}C levels requires further study.
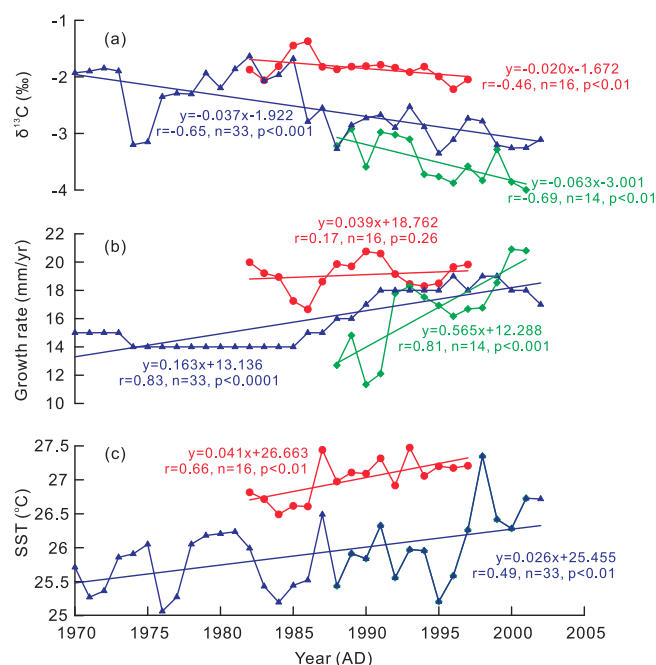

Fig. 2. Temporal variations of: (a) modern coral δ^{13}C time series, (b) modern coral growth rate time series, and (c) instrumental SST records at sampling locations. The instrumental SST records at the modern coral OC03 sampling location overlay those of the modern coral QG5 between 1988 and 2001 AD because they are both from the National Marine Observatory Station at Qinglan (Sun et al., 2008). The blue lines with solid triangle symbols, the green lines with solid square symbols, and the red lines with solid circle symbols represent the data for modern corals OC03, QG5, and XD4, respectively. (For interpretation of the references to color in this figure legend, the reader is referred to the web version of this article.)
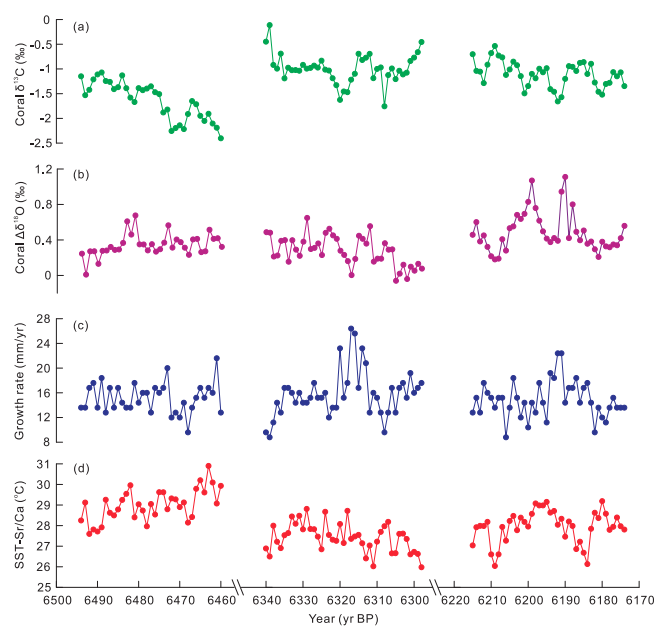
Fig. 3. Temporal variations of (a) δ^{13}C, (b) growth rate, (c) $\Delta\delta^{18}$O records of mid-Holocene corals, and (d) SST records reconstructed from coral Sr/Ca ratios. The growth periods of the mid-Holocene corals were 6174–6125, 6298–6340, and 6460–6494 yr BP for SYL-4, SYL-1-3, and SYO-15, respectively.

The annual mean δ^{13}C of the modern corals OC3 and XD4 showed statistically significant correlations with their annual growth rates over the study period (for OC3, r = −0.66, n = 33, p
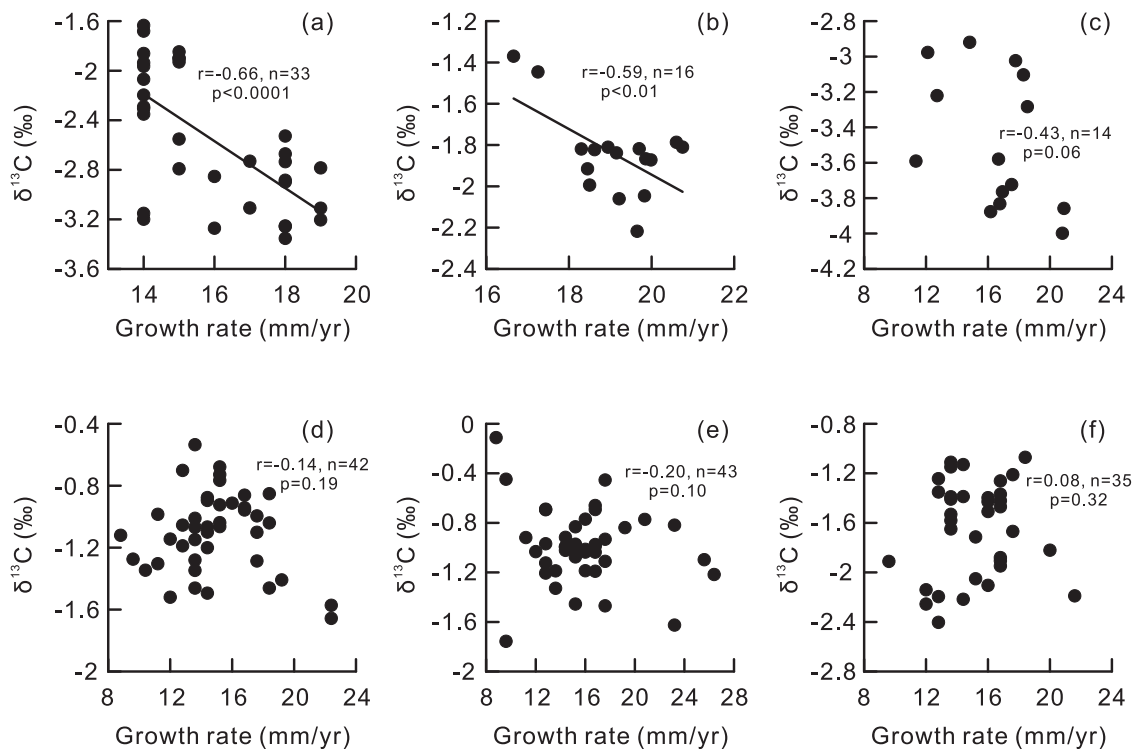
Fig. 4. Relationships between annual growth rate and $\delta^{13}C$ of the modern corals (*upper panel*) and the mid-Holocene corals (*lower panel*) for (a) OC03, (b) XD4, (c) QG5, (d) SYL-4, (e) SYL-1-3, and (f) SYO-15. Significant correlations are shown by regression lines.

< 0.0001, Fig. 4a; for XD4, $r = -0.59$, $n = 16$, $p < 0.01$, Fig. 4b). However, these correlations are not particularly convincing. It looks like that the significant correlation for OC3 is driven by the high density of points with the same growth rate, and that for XD4 is caused by the two points with relatively slow growth rates. Moreover, the correlation between the annual mean $\delta^{13}C$ and growth rate of the modern coral QG5 was weaker and not significant ($r = -0.43$, $n = 14$, $p = 0.06$, Fig. 4c). Such results suggest that the growth-rate-related kinetic isotope fractionation effect on annual resolution $\delta^{13}C$ levels preserved in modern SCS corals may be limited, site- and/or colony-specific, although some studies have indicated that the coral skeletal $\delta^{13}C$ is sensitivity to growth rate (e.g. Linsley et al., 2019). In addition, the strong time offsets between seasonal $\delta^{13}C$ and $\delta^{18}O$ series of the three corals indicated that the kinetic effect from equilibrium for both $\delta^{13}C$ and $\delta^{18}O$ appears to be fairly constant and the variations in their skeleton $\delta^{13}C$ might be driven mainly by metabolic effects (Sun et al., 2008).

As for the three mid-Holocene corals, there were no significant correlations between their annual mean $\delta^{13}C$ and growth rate (for SYL-4, $r = -0.14$, $n = 42$, $p = 0.19$, Fig. 4d; for SYL-1-3, $r = -0.20$, $n = 43$, $p = 0.10$, Fig. 4e; for SYO-15, $r = 0.08$, $n = 35$, $p = 0.32$, Fig. 4f). Therefore, the effect of growth rate on the variations in annual resolution $\delta^{13}C$ levels of the mid-Holocene corals studied here may be limited.

Based on the different correlations between coral $\delta^{13}C$ and growth rate, we infer that the responses of coral $\delta^{13}C$ to the kinetic isotope fractionation effect related to growth rate were different during the mid-Holocene and at the present. The major source of coral skeletal $CaCO_3$ deposition is metabolic CO_2 (Goreau and Yonge, 1977; Erez, 1978; Furla et al., 2000), so these differing responses of annual resolution $\delta^{13}C$ to growth rate may indicate that the main carbon source and/or its utilization process during calcification in coral reefs differed between the mid-Holocene and the present-day. This difference might be related to the changing levels of biological activity associated with the changes in climatic and environmental conditions such as the change of DIC pool by anthropogenic CO_2.

4.2. Temperature-dependent changes in coral $\delta^{13}C$

Some studies have suggested that SST may affect seasonal coral $\delta^{13}C$ by influencing the photosynthesis of symbiotic zooxanthellae (McConnaughey, 1989; Swart et al., 1996), but no correlation has been found between skeletal $\delta^{13}C$ and temperature in temperature-controlled experiments (Suzuki et al., 2005). Even so, studies of the relationship between modern coral $\delta^{13}C$ and SST over longer timescales remain scarce, as do those that focus on fossil corals.

As for the modern corals analyzed here, the negative correlations between annual coral $\delta^{13}C$ and SST were weak but significant (for OC3, $r = -0.29$, $n = 33$, $p = 0.05$; for XD4, $r = -0.46$, $n = 16$, $p = 0.04$; for QG5, $r = -0.26$, $n = 14$, $p = 0.05$). In addition, they show inverse decadal variations. The SSTs at the sampling sites increased gradually, but the $\delta^{13}C$ for all three modern corals declined progressively over the study period (Fig. 2). As intensification of respiration generally reduces coral $\delta^{13}C$ values (McConnaughey, 1989; McConnaughey et al., 1997) and the coral becomes more active when the temperature increases (Al-Horani, 2005), these inverse trends between decadal coral $\delta^{13}C$ and SST can be ascribed to intensified coral respiration caused by the rising temperature, and there should be a long-term declining trend in coral $\delta^{13}C$ variation due to global warming (Sun et al., 2008). Besides, the oceanic Suess effect associated with anthropogenic CO_2 emissions has made a significant contribution to the secular declining trend in coral $\delta^{13}C$ levels over the past 200 years (Swart et al., 2010; Deng et al., 2017). Therefore, it is possible that the negative correlations between the modern coral $\delta^{13}C$ and SST are the results of the Suess effect and the global warming. This hypothesis can be tested by the results of reanalyzing the relationship between the detrended modern coral $\delta^{13}C$ and SST time series. There is no significant negative

correlation between the two detrended time series of the three modern corals (for OC3, r = 0.23, n = 33, p = 0.10, Fig. 5a; for XD4, r = −0.24, n = 16, p = 0.19, Fig. 5b; for QG5, r = 0.25, n = 14, p = 0.19, Fig. 5c).

The study of mid-Holocene corals may help to thoroughly understand the control of SST on δ^{13}C because the concentration of atmospheric CO_2 was much lower, but the SST was higher during that period than at present (Monnin, 2006; Wei et al., 2007). The coral δ^{13}C series analyzed here all have significant negative correlations with SST during the mid-Holocene (for SYL-4, r = −0.51, n = 42, p < 0.001, Fig. 5d; for SYL-1-3, r = −0.46, n = 43, p < 0.01, Fig. 5e; for SYO-15, r = −0.52, n = 35, p < 0.001, Fig. 5f; for all, r = −0.70, n = 120, p < 0.0001, Fig. 5g). The negative correlation between coral δ^{13}C and SST should not be explained only by the intensified coral respiration caused by the rising temperature because the photosynthesis of endosymbiotic zooxanthellae is also temperature dependent at appropriate temperature range (Al-Horani, 2005). Photosynthesis of endosymbiotic zooxanthellae preferentially consumes $^{12}CO_2$, resulting in ^{13}C enrichment of the DIC in the internal calcification pool (Swart, 1983; McConnaughey, 1989; Grottoli and Welling-ton, 1999), so higher temperatures may enhance zooxanthellae photosynthesis and result in higher coral δ^{13}C (Swart et al., 1996). Therefore, the enhancements of respiration and photosynthesis resulting from rising temperatures have counteracting effects on coral δ^{13}C, and their combined effect should be considered when discussing the relationship between coral δ^{13}C and SST.

The ratio of photosynthesis to respiration (P/R) has been used to examine variations in coral δ^{13}C (Swart, 1983; Swart et al., 1996; Reynaud-Vaganay et al., 2001; Schoepf et al., 2014). During periods when the coral experiences a relatively high P/R ratio, corals will produce skeletons with relatively high δ^{13}C values, but during periods when there is a low P/R, the skeletons may be lower in δ^{13}C (Swart, 1983). In addition, photosynthetic activity of heat-stressed corals will drastically reduce due to the decreases of population density of the zooxanthellae (Hoegh-Guldberg and Smith, 1989), and respiration rates increase with increasing temperature in that coral become more active when the temperature increase (Al-Horani, 2005); and moreover, P/R ratios are significantly and negatively related to temperature (Coles and Jokiel, 1977; Stambler and Dubinsky, 2004; Scheufen et al., 2017). From these viewpoints, the significant negative correlations between coral δ^{13}C and SST during the mid-Holocene may be related to the variations in P/R caused by SST. The rising temperature would lead to a decrease in P/R and thereby the decline in coral δ^{13}C. The higher average annual temperature period around 6494–6460 yr BP ($\sim$29.00 ± 0.78 °C) had an average total coral δ^{13}C of −1.64 ± 0.38‰, which is much lower than the values from the periods 6340–6298 ($\sim$27.42 ± 0.70 °C) and 6215–6174 yr BP ($\sim$27.96 ± 0.79 °C) when temperatures were relatively low (−0.99 ± 0.30‰ and −1.10 ± 0.26‰, respectively, for their δ^{13}C averages). This difference also indicates that the variations in the metabolic P/R ratio might be responsible for the temperature-dependent changes in annual resolution coral δ^{13}C. It should be noted that the average δ^{13}C of each modern corals (−2.55 ± 0.55‰, −1.84 ± 0.20‰ and −3.48 ± 0.38‰ for OC3, XD4 and QG5, respectively) are more negative than those of mid-Holocene corals, although they were all collected around the Hainan Island. The much more negative δ^{13}C values in modern corals may result from the oceanic ^{13}C Suess effect (Swart et al., 2010; Deng et al., 2017).

Another possible explanation for the temperature-dependent changes in mid-Holocene coral δ^{13}C is that higher temperatures enhance the decomposition of terrestrial organic matter and deliver river water with higher DIC concentrations and more negative δ^{13}C levels to coastal regions, and thereby lead to the

negative coral δ^{13}C. DIC in terrestrial river water usually has a more negative δ^{13}C than that in seawater (Raich and Schlesinger, 1992; Moyer et al., 2012). In addition, the δ^{13}C of DIC and the river water temperature exhibit a striking negative correlation in South China, and the δ^{13}C of DIC during warmer periods is generally more negative than during colder periods (Jiao et al., 2008; Jia et al., 2012). When this DIC is transported to coastal regions by river water, the δ^{13}C of seawater DIC becomes more negative, resulting in a more negative coral δ^{13}C. Previous studies have demonstrated that the seasonal changes in coral δ^{13}C from coastal regions, like the sampling site of the mid-Holocene corals in this study, are controlled mainly by terrestrial carbon input, and are significantly influenced by terrestrial river runoff (Moyer and Grottoli, 2011; Moyer et al., 2012; Deng et al., 2013). The effect of terrestrial DIC on the annual coral δ^{13}C can be evaluated using the coral $\Delta\delta^{18}$O which is a proxy for river runoff (Moyer and Grottoli, 2011; Moyer et al., 2012; Deng et al., 2013). If the annual changes in coral δ^{13}C were mainly controlled by the ter-restrial DIC input, there should be significant positive correlations between the annual coral $\Delta\delta^{18}$O and δ^{13}C records. However, the correlations between the annual coral $\Delta\delta^{18}$O and δ^{13}C records (for SYL-4, r = −0.23, n = 42, p = 0.07, Fig. 6a; for SYL-1-3, r = 0.18, n = 43, p = 0.12, Fig. 6b; for SYO-15, r = −0.23, n = 35, p = 0.10, Fig. 6c; for all, r = 0.05, n = 120, p = 0.30, Fig. 6d) indicate that the terrestrial DIC input should not be the main control on the annual changes in coral δ^{13}C.

4.3. Possible effect of total solar irradiation on coral δ^{13}C

A recent study suggested that the variations in coral δ^{13}C over centennial timescales were controlled by total solar irradi-ation (TSI) via the photosynthetic activity of the endosymbiotic zooxanthellae during the Medieval Warm Period and Little Ice Age, but affected by the oceanic Suess effect during the Current Warm Period (Deng et al., 2017). The concentration of atmo-spheric CO_2 during the mid-Holocene was much lower than at present and remained relatively stable (Monnin, 2006), so the effect of the transfer of CO_2 from the atmosphere into the sur-face oceans on the variations in coral δ^{13}C may not have been significant, but the role of TSI may still be important. Coral δ^{13}C and reconstructed TSI based on the cosmogenic radionuclide ^{10}Be record in ice cores (Steinhilber et al., 2009) for the mid-Holocene generate roughly similar variation profiles (Fig. 7), and the sig-nificant $\sim$11-year cycles in three coral δ^{13}C time series may be associated with the 11-year periodicity of solar activity (Balogh et al., 2014) (Fig. 8). The differences in their variations might result from the low resolution of TSI record and/or the dating errors for corals and ice cores. If the differences were free from these factors, then they may mean that the variations in coral δ^{13}C cannot be interpreted using only the photosynthesis of en-dosymbiotic zooxanthellae even though its role cannot be denied. Therefore, the combined effect of photosynthesis and respiration should be more reasonable to study the underlying mechanism of temperature-dependent changes in fossil annual resolution coral δ^{13}C.

5. Conclusions

Annual-resolution δ^{13}C series in both modern and fossil corals from the SCS were studied to explore the biological and climatic significance of coral δ^{13}C during the mid-Holocene. The main conclusions were as follows.

(1) For modern corals, the growth-rate-related kinetic isotope effect on their annual resolution δ^{13}C may be limited, site- and/or colony-specific; and their δ^{13}C levels and SST have an inverse
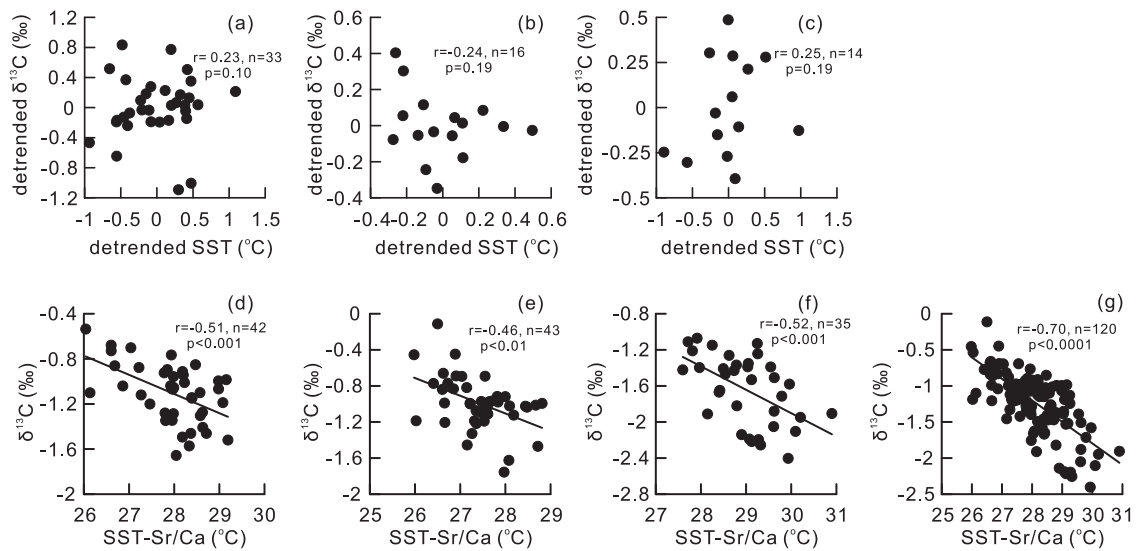
Fig. 5. Relationships between annual SST and $\delta^{13}C$ of the modern corals (*upper panel*) and the mid-Holocene corals (*lower panel*) for (a) OC03, (b) XD4, (c) QG5, (d) SYL-4, (e) SYL-1-3, (f) SYO-15, and (g) all data from three mid-Holocene corals. The modern SST and $\delta^{13}C$ time series were detrended to remove the effects of global warming and Suess effect, respectively. Significant correlations are shown by regression lines.
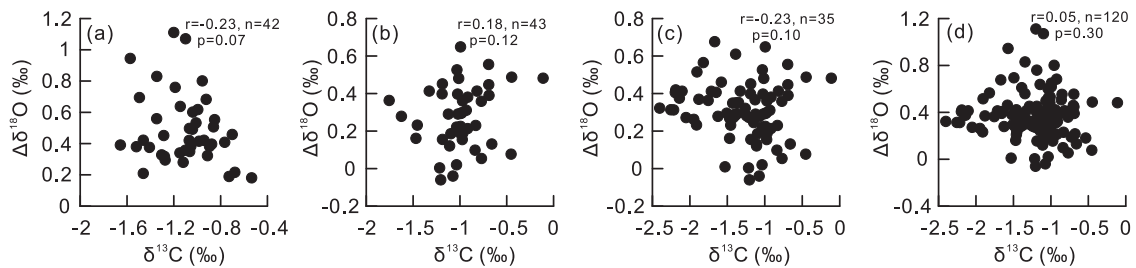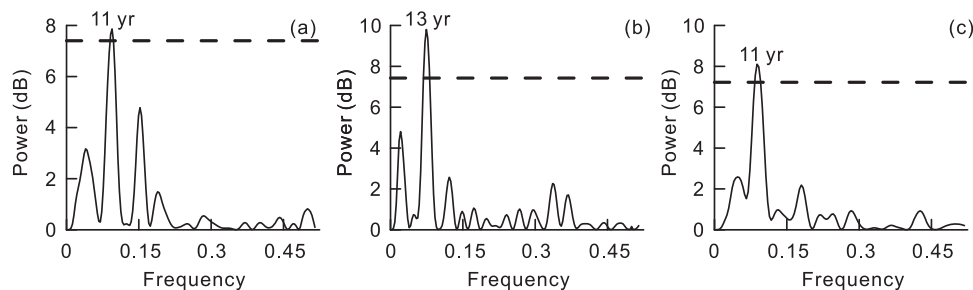

Fig. 6. Relationships between annual $\Delta\delta^{18}O$ and $\delta^{13}C$ of the mid-Holocene corals. (a) SYL-4, (b) SYL-1-3, (c) SYO-15 and (d) all data from three mid-Holocene corals.
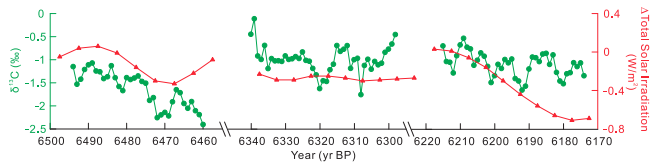
Fig. 7. Temporal variations of mid-Holocene coral $\delta^{13}C$ (the green lines with solid circle symbols) and total solar irradiance (TSI; red lines with solid triangles) reconstructed from an observationally derived relationship between TSI and the open solar magnetic field (Steinhilber et al., 2009) during the mid-Holocene. (For interpretation of the references to color in this figure legend, the reader is referred to the web version of this article.)

relationship over decadal timescales, suggesting the influence of complicated controlling factors on modern coral $\delta^{13}C$ levels.

(2) For mid-Holocene corals, the effect of the kinetic isotope effect on mid-Holocene annual resolution coral $\delta^{13}C$ variations is also not obvious. Coral $\delta^{13}C$ and reconstructed TSI have only roughly similar variation profiles, which might result from the low resolution of TSI record and/or the dating errors. However, annual resolution coral $\delta^{13}C$ shows temperature-dependent changes over the studied periods during 6100–6500 yr BP.

(3) The significant negative correlation between coral $\delta^{13}C$ and SST is a manifestation of coral response to mid-Holocene thermal stress. Usually, coral $\delta^{13}C$ and P/R ratios are positively related, but P/R is significantly and negatively related to temperature under the high temperature conditions in that photosynthetic activity of heat-stressed corals will drastically reduce due to the decreases of population density and photosynthetic rate of the zooxanthellae.

Fig. 8. Simple periodogram analysis of the mid-Holocene coral $\delta^{13}C$ time series using the PAST software (Hammer et al., 2001). (a) SYL-4, (b) SYL-1-3 and (c) SYO-15. The dashed lines indicate the 95% confidence intervals. Numbers represent the periodicities of the peaks.

Declaration of competing interest

The authors declare that they have no known competing financial interests or personal relationships that could have appeared to influence the work reported in this paper.

Acknowledgments

Appendix A. Supplementary data

Supplementary material related to this article can be found online at https://doi.org/10.1016/j.rsma.2019.100950.

References

Al-Horani, F., 2005. Effects of changing seawater temperature on photosynthesis and calcification in the scleractinian coral *Galaxea fascicularis*, measured with O_2, Ca^{2+} and pH microsensors. Sci. Mar. 69, 347–354.

Allison, N., Tudhope, A.W., Fallick, A.E., 1996. Factors influencing the stable carbon and oxygen isotopic composition of *Porites lutea* coral skeletons from Phuket, South Thailand. Coral Reefs 15, 43–57.

Axford, Y., Losee, S., Briner, J.P., Francis, D.R., Langdon, P.G., Walker, I.R., 2013. Holocene temperature history at the western Greenland Ice Sheet margin reconstructed from lake sediments. Quat. Sci. Rev. 59, 87–100.

Bâki Iz, H., 2018. Is the global sea surface temperature rise accelerating? Geode. Geodyn. 9, 432–438.

Balogh, A., Hudson, H.S., Petrovay, K., von Steiger, R., 2014. Introduction to the solar activity cycle: overview of causes and consequences. Space Sci. Rev. 186, 1–15.

Buddemeier, R.W., Jokiel, P.L., Zimmerman, K.M., Lane, D.R., Carey, J.M., Bohling, G.C., Martinich, J.A., 2008. A modeling tool to evaluate regional coral reef responses to changes in climate and ocean chemistry. Limnol. Oceanogr. Methods 6, 395–411.

Camp, E.F., Schoepf, V., Mumby, P.J., Hardtke, L.A., Rodolfo-Metalpa, R., Smith, D.J., Suggett, D.J., 2018. The future of coral reefs subject to rapid climate change: Lessons from natural extreme environments. Front. Mar. Sci. 5 (4), http://dx.doi.org/10.3389/fmars.2018.00004.

Carpenter, K.E., Abrar, M., Aeby, G., Aronson, R.B., Banks, S., Bruckner, A., Chiriboga, A., Cortés, J., Delbeek, J.C., DeVantier, L., Edgar, G.J., Edwards, A.J., Fenner, D., Guzmán, H.M., Hoeksema, B.W., Hodgson, G., Johan, O., Licuanan, W.Y., Livingstone, S.R., Lovell, E.R., Moore, J.A., Obura, D.O., Ochavillo, D., Polidoro, B.A., Precht, W.F., Quibilan, M.C., Reboton, C., Richards, Z.T., Rogers, A.D., Sanciangco, J., Sheppard, A., Sheppard, C., Smith, J., Stuart, S., Turak, E., Veron, J.E.N., Wallace, C., Weil, E., Wood, E., 2008. One-third of reef-building corals face elevated extinction risk from climate change and local impacts. Science 321, 560–563.

Chen, T., Li, S., Shi, Q., Chen, T., 2016. Cold tolerance of subtropical Porites lutea from the northern South China Sea. Acta Oceanol. Sin. 35, 58–64.

Chen, T., Roff, G., McCook, L., Zhao, J., Li, S., 2018. Recolonization of marginal coral reef flats in response to recent sea-level rise. J. Geophys. Res. Oceans 123, 7618–7628.

Coles, S.L., Jokiel, P.L., 1977. Effects of temperature on photosynthesis and respiration in hermatypic corals. Mar. Biol. 43, 209–216.

Dassié, E.P., Lemley, G.M., Linsley, B.K., 2013. The suess effect in Fiji coral $\delta^{13}C$ and its potential as a tracer of anthropogenic CO_2 uptake. Palaeogeogr. Palaeoclimatol. Palaeoecol. 370, 30–40.

DeCarlo, T.M., Comeau, S., Cornwall, C.E., McCulloch, M.T., 2018. Coral resistance to ocean acidification linked to increased calcium at the site of calcification. Proc. R. Soc. B-Biol. Sci. 285, 20180564.

Deng, W., Chen, X., Wei, G., Zeng, T., Zhao, J.-x., 2017. Decoupling of coral skeletal $\delta^{13}C$ and solar irradiance over the past millennium caused by the oceanic Suess effect. Paleoceanography 32, 161–171.

Deng, W., Wei, G., Li, X., Yu, K., Zhao, J.-x., Sun, W., Liu, Y., 2009. Paleoprecipitation record from coral Sr/Ca and d18O during the mid Holocene in the northern South China Sea. Holocene 19, 811–821.

Deng, W., Wei, G., Xie, L., Yu, K., 2013. Environmental controls on coral skeletal $\delta^{13}C$ in the northern South China Sea. J. Geophys. Res. Biogeosci. 118, 1359–1368.

Erez, J., 1978. Vital effect on stable-isotope composition seen in foraminifera and coral skeletons. Nature 273, 199–202.

Furla, P., Galgani, I., Durand, I., Allemand, D., 2000. Sources and mechanisms of inorganic carbon transport for coral calcification and photosynthesis. J. Exp. Biol. 203, 3445–3457.

Gagan, M.K., Ayliffe, L.K., Hopley, D., Cali, J.A., Mortimer, G.E., Chappell, J., McCulloch, M.T., Head, M.J., 1998. Temperature and surface-ocean water balance of the mid-Holocene tropical Western Pacific. Science 279, 1014–1018.

Gagan, M.K., Chivas, A.R., Isdale, P.J., 1994. High-resolution isotopic records from corals using ocean temperature and mass-spawning chronometers. Earth Planet. Sci. Lett. 121, 549–558.

Goreau, T.J., Yonge, M., 1977. Coral skeletal chemistry: physiological and environmental regulation of stable isotopes and trace metals in *Montastrea annularis*. Proc. R. Soc. B-Biol. Sci. 196, 291–315.

Grottoli, A.G., 2000. Stable carbon isotopes ($\delta^{13}C$) in coral skeletons. Oceanography 13, 93–97.

Grottoli, A.G., Wellington, G.M., 1999. Effect of light and zooplankton on skeletal $\delta^{13}C$ values in the eastern Pacific corals *Pavona clavus* and *Pavona gigantea*. Coral Reefs 18, 29–41.

Guo, Y., Deng, W., Chen, X., Wei, G., Yu, K., Zhao, J.-x., 2016. Saltier sea surface water conditions recorded by multiple mid-Holocene corals in the northern South China Sea. J. Geophys. Res. Oceans 632, 3–6330.

Gustafson, S.K., 2006. Assessment of Image Analysis as a Measure of Scleractinian Coral Growth (Masters thesis). University of South Florida, St. Petersburg, Florida.

Hammer, Ø., Harper, D.A.T., Ryan, P.D., 2001. PAST: Paleontological statistics software package for education and data analysis. Palaeontol. Electron. 4, 1–9.

Hewitt, C.D., Mitchell, J.F.B., 1998. A fully coupled GCM simulation of the climate of the mid Holocene. Geophys. Res. Lett. 25, 361–364.

Hoegh-Guldberg, O., Mumby, P.J., Hooten, A.J., Steneck, R.S., Greenfield, P., Gomez, E., Harvell, C.D., Sale, P.F., Edwards, A.J., Caldeira, K., Knowlton, N., Eakin, C.M., Iglesias-Prieto, R., Muthiga, N., Bradbury, R.H., Dubi, A., Hatziolos, M.E., 2007. Coral reefs under rapid climate change and ocean acidification. Science 318, 1737–1742.

Hoegh-Guldberg, O., Poloczanska, E.S., Skirving, W., Dove, S., 2017. Coral reef ecosystems under climate change and ocean acidification. Front. Mar. Sci. 4 (158), http://dx.doi.org/10.3389/fmars.2017.00158.

Hoegh-Guldberg, O., Smith, G.J., 1989. The effect of sudden changes in temperature, light and salinity on the population density and export of zooxanthellae from the reef corals *stylophora pistillata* Esper and *seriatopora hystrix* Dana. J. Exp. Mar. Biol. Ecol. 129, 279–303.

Hughes, T.P., Kerry, J.T., Álvarez Noriega, M., Álvarez Romero, J.G., Anderson, K.D., Baird, A.H., Babcock, R.C., Beger, M., Bellwood, D.R., Berkelmans, R., Bridge, T.C., Butler, I.R., Byrne, M., Cantin, N.E., Comeau, S., Connolly, S.R., Cumming, G.S., Dalton, S.J., Diaz-Pulido, G., Eakin, C.M., Figueira, W.F., Gilmour, J.P., Harrison, H.B., Heron, S.F., Hoey, A.S., Hobbs, J.-P.A., Hoogenboom, M.O., Kennedy, E.V., Kuo, C.-y., Lough, J.M., Lowe, R.J., Liu, G., McCulloch, M.T., Malcolm, H.A., McWilliam, M.J., Pandolfi, J.M., Pears, R.J., Pratchett, M.S., Schoepf, V., Simpson, T., Skirving, W.J., Sommer, B., Torda, G., Wachenfeld, D.R., Willis, B.L., Wilson, S.K., 2017. Global warming and recurrent mass bleaching of corals. Nature 543 (373).

Jia, G.D., Chen, F.J., Deng, W.F., 2012. Seasonal variations of dissolved inorganic carbon isotope in the Beijiang River. Earth Sci.-J. China. Univ. Geosci. 37, 365–369.

Jiao, S.L., Tao, Z., Gao, Q.Z., Liu, K., She, J.W., Ding, J., Liu, Z.F., 2008. Stable isotopic composition of riverine dissolved inorganic carbon in the Xijiang River Inner Estuary. J. Geogr. Sci. 18, 363–372.

Kittinger, J.N., Pandolfi, J.M., Blodgett, J.H., Hunt, T.L., Jiang, H., Maly, K., McClenachan, L.E., Schultz, J.K., Wilcox, B.A., 2011. Historical reconstruction reveals recovery in Hawaiian coral reefs. PLoS One 6, e25460.

Knowlton, N., Brainard, R.E., Fisher, R., Moews, M., Plaisance, L., Caley, M.J., 2010. Coral reef biodiversity. In: McIntyre, A.D. (Ed.), Life in the World'S Oceans. Wiley-Blackwell, Oxford.

Lam, V.W.Y., Chavanich, S., Djoundourian, S., Dupont, S., Gaill, F., Holzer, G., Isensee, K., Katua, S., Mars, F., Metian, M., Hall-Spencer, J.M., 2019. Dealing with the effects of ocean acidification on coral reefs in the Indian Ocean and Asia. Reg. Stud. Mar. Sci. 28, 100560.

Linsley, B.K., Dunbar, R.B., Dassié, E.P., Tangri, N., Wu, H.C., Brenner, L.D., Wellington, G.M., 2019. Coral carbon isotope sensitivity to growth rate and water depth with paleo-sea level implications. Nat. Commun. 10 (2056).

Liu, Y., Liu, W., Peng, Z., Xiao, Y., Wei, G., Sun, W., He, J., Liu, G., Chou, C.-L., 2009. Instability of seawater pH in the South China Sea during the mid-late Holocene: Evidence from boron isotopic composition of corals. Geochim. Cosmochim. Acta 73, 1264–1272.

Liu, Y., Peng, Z., Zhou, R., Song, S., Liu, W., You, C.-F., Lin, Y.-P., Yu, K., Wu, C.-C., Wei, G., Xie, L., Burr, G.S., Shen, C.-C., 2014. Acceleration of modern acidification in the South China Sea driven by anthropogenic CO_2. Sci. Rep. 4 (5148).

Lough, J.M., Llewellyn, L.E., Lewis, S.E., Turney, C.S.M., Palmer, J.G., Cook, C.G., Hogg, A.G., 2014. Evidence for suppressed mid-Holocene northeastern Australian monsoon variability from coral luminescence. Paleoceanography 29, 581–594.

McConnaughey, T.A., 1989. ^{13}C and ^{18}O isotopic disequilibrium in biological carbonates: I. Patterns. Geochim. Cosmochim. Acta 53, 151–162.

McConnaughey, T.A., Burdett, J., Whelan, J.F., Paull, C.K., 1997. Carbon isotopes in biological carbonates: Respiration and photosynthesis. Geochim. Cosmochim. Acta 61, 611–622.

McCulloch, M.T., D'Olivo, J.P., Falter, J., Holcomb, M., Trotter, J.A., 2017. Coral calcification in a changing World and the interactive dynamics of pH and DIC upregulation. Nat. Commun. 8 (15686), http://dx.doi.org/10.1038/ncomms15686.

McCulloch, M., Falter, J., Trotter, J., Montagna, P., 2012. Coral resilience to ocean acidification and global warming through pH up-regulation. Nat. Clim. Change 2, 623–627.

Monnin, E., 2006. EPICA DOme C high resolution carbon dioxide concentrations. Retrieved from: https://doi.org/10.1594/PANGAEA.472488.

Moyer, R.P., Grottoli, A.G., 2011. Coral skeletal carbon isotopes (δ^{13}C and Δ^{14}C) record the delivery of terrestrial carbon to the coastal waters of Puerto Rico. Coral Reefs 30, 791–802.

Moyer, R.P., Grottoli, A.G., Olesik, J.W., 2012. A multiproxy record of terrestrial inputs to the coastal ocean using minor and trace elements (Ba/Ca, Mn/Ca, Y/Ca) and carbon isotopes (δ^{13}C, Δ^{14}C) in a nearshore coral from Puerto Rico. Paleoceanography 27, PA3205.

Okai, T., Suzuki, A., Kawahata, H., Terashima, S., Imai, N., 2012. Preparation of a new Geological Survey of Japan geochemical reference material: coral jcp-1. Geostandards Newsletter 26, 95–99.

Raich, J.W., Schlesinger, W.H., 1992. The global carbon dioxide flux in soil respiration and its relationship to vegetation and climate. Tellus B 44, 81–99.

Reynaud-Vaganay, S., Juillet-Leclerc, A., Jaubert, J., Gattuso, J.P., 2001. Effect of light on skeletal δ^{13}C and δ^{18}O, and interaction with photosynthesis, respiration and calcification in two zooxanthellate scleractinian corals. Palaeogeogr. Palaeoclimatol. Palaeoecol. 175, 393–404.

Samartin, S., Heiri, O., Joos, F., Renssen, H., Franke, J., Brönnimann, S., Tinner, W., 2017. Warm Mediterranean mid-Holocene summers inferred from fossil midge assemblages. Nat. Geosci. 10 (207).

Scheufen, T., Krämer, W.E., Iglesias-Prieto, R., Enríquez, S., 2017. Seasonal variation modulates coral sensibility to heat-stress and explains annual changes in coral productivity. Sci. Rep. 7 (4937).

Schoepf, V., Levas, S.J., Rodrigues, L.J., McBride, M.O., Aschaffenburg, M.D., Matsui, Y., Warner, M.E., Hughes, A.D., Grottoli, A.G., 2014. Kinetic and metabolic isotope effects in coral skeletal carbon isotopes: A re-evaluation using experimental coral bleaching as a case study. Geochim. Cosmochim. Acta 146, 164–178.

Shi, Y., Kong, Z., Wang, S., Tang, L., Wang, F., Yao, T., Zhao, X., Zhang, P., Shi, S., 1993. Mid-holocene climates and environments in China. Glob. Planet. Change 7, 219–233.

Stambler, N., Dubinsky, Z., 2004. Stress effects on metabolism and photosynthesis of hermatypic corals. In: Rosenberg, E., Loya, Y. (Eds.), Coral Health and Disease. Springer Berlin Heidelberg, Berlin, Heidelberg, pp. 195–215.

Steinhilber, F., Beer, J., Fröhlich, C., 2009. Total solar irradiance during the Holocene. Geophys. Res. Lett. 36, http://dx.doi.org/10.1029/2009GL040142.

Su, R., Lough, J.M., Sun, D., 2016. Variations in massive porites growth rates at Hainan Island northern South China Sea. Mar. Ecol. Prog. Ser. 546, 47–60.

Sun, D., Su, R., McConnaughey, T.A., Bloemendal, J., 2008. Variability of skeletal growth and δ^{13}C in massive corals from the South China Sea: Effects of photosynthesis, respiration and human activities. Chem. Geol. 255, 414–425.

Suzuki, A., Hibino, K., Iwase, A., Kawahata, H., 2005. Intercolony variability of skeletal oxygen and carbon isotope signatures of cultured Porites corals: Temperature-controlled experiments. Geochim. Cosmochim. Acta 69, 4453–4462.

Swart, P.K., 1983. Carbon and oxygen isotope fractionation in scleractinian corals: a review. Earth-Sci. Rev. 19, 51–80.

Swart, P.K., Greer, L., Rosenheim, B.E., Moses, C.S., Waite, A.J., Winter, A., Dodge, R.E., Helmle, K., 2010. The ^{13}C Suess effect in scleractinian corals mirror changes in the anthropogenic CO_2 inventory of the surface oceans. Geophys. Res. Lett. 37 (L05604), http://dx.doi.org/10.1029/2009gl041397.

Swart, P.K., Leder, J.J., Szmant, A.M., Dodge, R.E., 1996. The origin of variations in the isotopic record of scleractinian corals: II. Carbon. Geochim. Cosmochim. Acta 60, 2871–2885.

Tanzil, J.T.I., Brown, B.E., Dunne, R.P., Lee, J.N., Kaandorp, J.A., Todd, P.A., 2013. Regional decline in growth rates of massive Porites corals in Southeast Asia. Glob. Change Biol. 19, 3011–3023.

Wei, G.J., Deng, W.F., Yu, K.F., Li, X.H., Sun, W.D., Zhao, J.X., 2007. Sea surface temperature records in the Northern South China Sea from mid-Holocene coral Sr/Ca ratios. Paleoceanography 22, PA3206. http://dx.doi.org/10.1029/2006PA001270.

Xu, S., Yu, K., Wang, Y., Liu, T., Jiang, W., Wang, S., Chu, M., 2018. Oil spill recorded by skeletal δ^{13}C of Porites corals in Weizhou Island, Beibu Gulf, Northern South China Sea. Estuar. Coast. Shelf Sci. 207, 338–344.

Yu, K.F., 2012. Coral reefs in the South China Sea: Their response to and records on past environmental changes. Sci. China-Earth Sci. 55, 1217–1229.